RSC Advances

ROYAL SOCIETY OF CHEMISTRY

www.rsc.org/advances

RSC Advances

COMMUNICATION

Tuning the surface properties of alloyed CdS_xSe_{1-x} 2D nanosheets

Pradipta Sankar Maiti[a] and Maya Bar-Sadan[a]

Received 00th January 20xx,
Accepted 00th January 20xx

DOI: 10.1039/x0xx00000x

www.rsc.org/

Low temperatures synthesis of CdS_xSe_{1-x} 2D nanosheets offers tuning of the optoelectronic properties by surface engineering. Analysis by ligand exchange revealed a Se-rich surface. By adjusting the reaction temperature, it was possible to control the surface passivation thus using the charge transfer to the ligands for reduced recombination and emission. These structures can be used for applications where fast recombination should be avoided, such as photocatalysis.

The recent progress in the synthesis of semiconducting colloidal 2D nanosheets with 1D quantum confinement has brought extensive research of their optical properties and the associated physical and photocatalytic phenomena.[1-5] Efficient charge transfer has been shown to occur between adjacent 4 monolayers and 5 monolayers CdSe nanoplatelets, demonstrating that the organic ligands covering the colloidal nanosheets are not an obstacle for their integration within vertically stacked devices.[4] The 2D morphology is appealing: the emergence of vdW solids has brought a surge in the attempts to develop production schemes for the realization of ultra-thin junctions by heterostructuring.[6-9] Another possible application is hydrogen evolution and water splitting, where intimate contact between Cd chalcogenides as the absorbers covered by a few layers of MoS_2 as the co-catalyst has shown enhanced activity.[10-13] The 2D geometry allows large interface area between the materials, thus promoting efficient and fast charge transfer between the layers. The small thickness is also advantageous in order to overcome the typical small charge carrier diffusion lengths in semiconductors, which hamper high yield photocatalytic water splitting.[14] However, these applications are strongly relying on surface engineering to optimize charge carrier life times by structural modification and ligand passivation.[15] Here, we use the delicate relation of the structure and the optical properties to explore and probe the surface of the alloyed nanosheets in order to correlate the reaction temperature with the surface composition and surface defects.

The 2D ultrathin cadmium chalcogenides are synthesized either in zinc blend[16] or wurtzite[17] phase by wet chemistry. So far, the remarkable optoelectronic properties of zinc blend Cd chalcogenides and especially CdSe nanoplatelets have focused the attention of the scientific community[18-20] and hybrid structures either in 'core-crown' or 'core-wing' forms were shown to dramatically alter the nanoplatelets optoelectronic properties.[21-24] The ultimate control over the thickness of the structures provides extremely narrow emission spectra, with FWHM as narrow as 7-10 nm,[5] making these structures especially suitable for opto-electronic devices such as light emitting diodes.

However, optoelectronic tuning of wurtzite 2D nanosheets was not explored extensively to date. Wurtzite 2D Cd chalcogenides were initially synthesized using a soft-template method.[25] The growth of the wurtzite 2D nanosheets is unique, since it is carried out in extremely low temperature regime (45-120°C), which is rare for the formation of semiconductor nanocrystals.[26] The detailed mechanism of formation revealed that the magic size CdSe nuclei (which serve as building blocks) and the annealing temperature play a crucial role in the formation mechanism.[26, 27] Recently, we have demonstrated continuous control over the composition of homogenously alloyed wurtzite CdS_xSe_{1-x} nanoplatelets and by that control over their optical properties i.e. the absorption and emission.[28, 29] We have used aberration corrected TEM to investigate the structure of the nanosheets on the atomic scale in order to understand their formation mechanism, concluding that a mechanism of oriented attachment of patches exists alongside a unidirectional growth of the anion–rich facet. The surface defects produced by this growth mechanism serve for trapping of excitons by the sites located at the CdSe nanoplatelet surface instead of the commonly resolved multi-particle Auger recombination mechanism,[30] making the surface sensitive to photo etching in contrast to

[a] Department of Chemistry and the Ilse Katz Institute Ben Gurion University, Beer-Sheva, 8410501, Israel, Email: barsadan@bgu.ac.il

Electronic Supplementary Information (ESI) available: Experimental details, EDS spectra (Figure S1), XRD (Figure S2) emission spectra under different excitation wavelength (Figure S3), emission spectra of pure *w*-CdSe nanosheets before and after modification with PPh_3 (Figure S4), UV-visible spectra after the ligand modification (Figure S5), emission spectra of *zb*-CdSe nanosheets before and after modification with 1-dodecanthiol (Figure S6) and emission spectra after the modification with 1-dodecanthiol (Figure S7).
See DOI: 10.1039/x0xx00000x

edge degradation, typical of the zinc blende structures.[31] In order to assess the prospect to utilize such structures for applications such as photocatalysis, there is a need to understand the effect of the atomic-scale surface structure and its passivating ligands on the optical properties.[15]

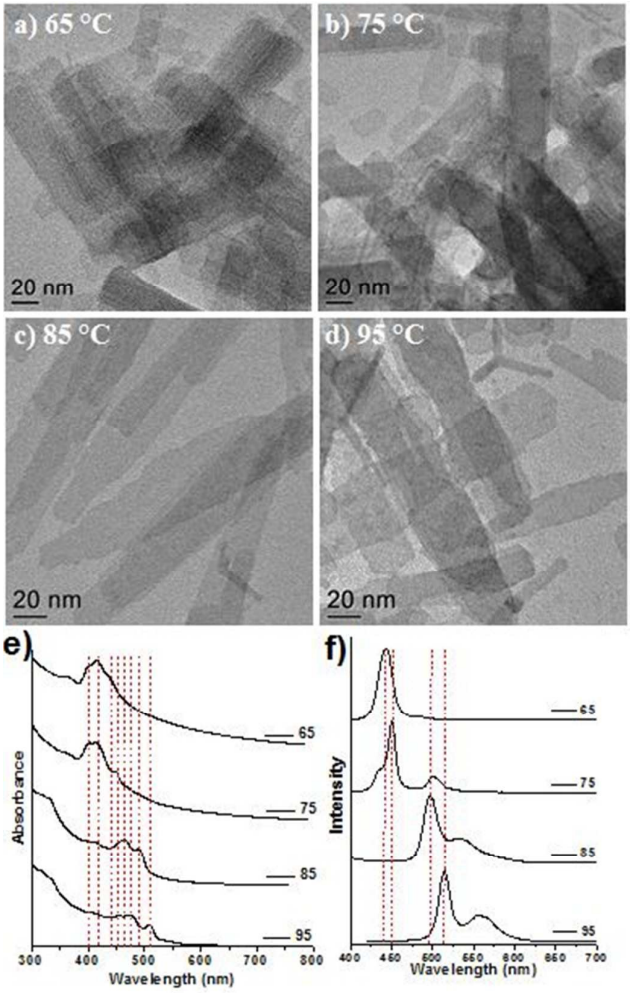

Figure 1 Transmission Electron Microscopy (TEM) images of the 2D CdS_xSe_{1-x} nanosheets synthesized at different temperatures (1a-d). Absorbance spectra (e) and corresponding photoluminescence spectra (f) of the CdS_xSe_{1-x} nanosheets as recorded in chloroform at room temperature.

The 2D alloyed CdS_xSe_{1-x} nanosheets were synthesized using a mixture of oleylamine and octylamine as the solvent.[28, 29, 32] Following the addition of the S-Se-$NaBH_4$ precursor, the reaction growth temperature was set to 65°C, 75°C, 85°C and 95°C, respectively, and kept for 10h (See Supporting Information for detailed protocols). TEM images of all the synthetic batches showed uniform contrast of the platelets, as seen in Figure 1a-d. The length of the structures varied from 80-120 nm, and their width was 30-40 nm. However, the structures produced in the lower temperatures (65-75 °C) showed uniform width and an overall rectangle shape with smooth edges, in contrast to the rough and irregular edges seen in the higher temperature structures.

Table 1 Variation of S and Se in the CdS_xSe_{1-x} nanosheets with temperature (by EDS analysis)

	65 °C	75 °C	85 °C	95 °C
S fraction (x)	0.41	0.37	0.30	0.20
Se fraction (1-x)	0.59	0.63	0.70	0.80

The challenge in synthesizing these 2D nanosheets is to control at the same time the uniformity of the thickness down to atomic dimensions, the perfection of the crystallographic structure and the composition. An addition of $NaBH_4$ is required to balance the different reactivities of the Se and S precursors.[28, 29] Se is the more reactive species and it existed in excess in the final product of all the samples, all of which were synthesized with a feed ratio of 1:1 Se:S. EDS analysis (Table 1 and Figure S1) presents the final composition of the structures. Increasing the temperature enhanced the incorporation of Se within the structures such that the final Se:S ratio was 4:1 for the synthesis at 95 °C compared with Se:S ratio of 1.4:1 for the synthesis at 65 °C. Our previous work has shown that in contrast to other synthetic protocols, the alloyed 2D nanosheets grow via oriented attachment under soft-templating conditions, resulting in a homogenous composition without S-rich and Se-rich areas.[28, 29] The homogenous composition promotes sharp emission peaks, whereas a composition gradient produces emission in a variety of wavelengths, thus degrading the optical quality of the samples. The crystal structure of the samples was examined by powder X-ray diffraction (XRD). All XRD patterns correspond to the hexagonal wurtzite phase (see Figure S2). Although all the samples were crystalline, higher synthesis temperature resulted in sharper peaks and in a shift towards the lower angles, due to the higher Se content. In addition, the broadening of the peak at the higher angles for the 65 °C may indicate thinner structures, i.e. 4 monolayers compared with those produced at the higher temperatures.

Optical absorbance and photoluminescence are a sensitive probe for the overall morphology as well as for the edges and surface structures. The UV-Vis absorption spectra of the CdS_xSe_{1-x} nanosheets and their corresponding photoluminescence (PL) spectra are shown in Figure 1e and f. The spectra are characteristic of 2D nanosheets showing 1D quantum confinement and all the excitonic peaks can be assigned to heavy-hole to electron and light-hole-electron transitions. The 1st excitonic transition for the lower Se-content (65°C) nanosheets was at 444 nm and at 517 nm for the highest Se-content (95°C), in accordance with the literature. Additional Se is known to red shift the absorbance and photoluminesence of CdS_xSe_{1-x} nanosheets,[20, 28, 29] CdS_xSe_{1-x} QD[33] and CdS_xSe_{1-x} nanowires.[34]

The normalized PL spectra of all the samples showed band-edge emission and narrow emission peak, with full width at half maximum (FWHM) as small as 19 nm at 444 nm for the synthesis temperature of 65°C and 16 nm at 517 nm for 95°C, indicating an extremely uniform thickness. Another evidence for the long-range uniform thickness is that the emission peak

maxima for individual batches are fixed even when excited at different wavelengths (see Figure S3). The shift of the PL peak to higher wavelengths may also indicate a combined effect of composition and morphology transition to thicker samples of 5 monolayers at 95°C compared to 4 monolayers at 65°C. The higher the synthesis temperature was, the more pronounced the low-energy emission peak was in the PL spectra, which we attribute to defects or structural disorder. From the TEM images of Figure 1a-d, the higher synthesis temperature produced edge irregularities rather than a rectangular stripe. Therefore, the extremely low synthesis temperature has yielded structures with improved optical properties which we attribute to the edge reconstruction.

In addition to the manipulation of the edge reconstruction, there is a need to focus on the surface passivation as well. Wurtzite structures are known to have surface defects on their basal planes[31] and this atomic-scale reconstruction of the interface significantly affects the optical properties of the material. A ligand effect may be the cause for the re-organization of the surface composition[35] or it may produce passivation of the surface and a decrease of the number of trap states.[15, 36]

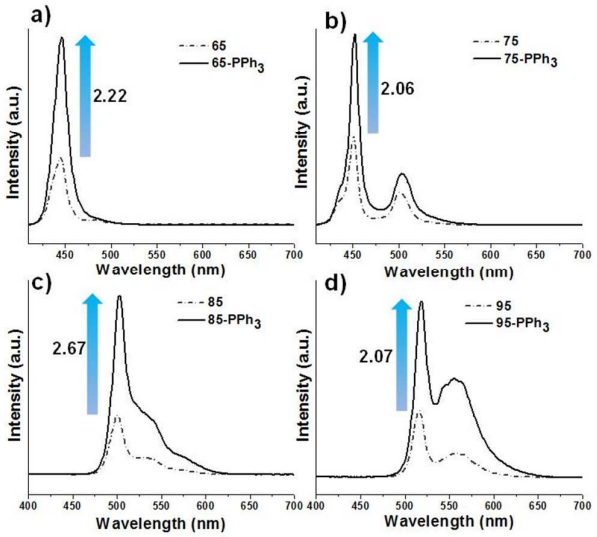

Figure 2 Photoluminescence spectra of 2D CdS_xSe_{1-x} nanosheets (a-d) before (dashed) and after (solid) functionalization with triphenylphosphine (TPP) as recorded at room temperature.

In order to probe the surface of the nanosheets we exchanged the amine ligands used for the synthesis by either tri-phenylphosphine (PPh_3) or dodecanethiol (DDT). Phosphines are a good probe for the Se content of the surfaces since it was shown to increase dramatically the PL of Se- rich surfaces while having almost no effect on Cd-rich surfaces.[37, 38] In our case, the addition of PPh_3 yielded approximately 2-fold increase of PL in all the samples (see Figure 2), indicating a Se-rich interface, in contrast to zinc blende nanoplatelets.[39] The observation of the excess Se on the wurtzite surface is inherent to our synthesis protocol and it was confirmed by similar experiments on pure CdSe nanosheets (see Figure S4). The increase of the overall PL signal is common to all the samples, but it also brings about an increase in the disorder peak seen at the higher wavelengths. The advantage of the low temperature synthesis, where no disorder peaks were observed, is then apparent. Changes in the structural features due to the ligand modification were excluded since the samples retained the optical absorbance spectra after the ligand exchange process (see Figure S5).

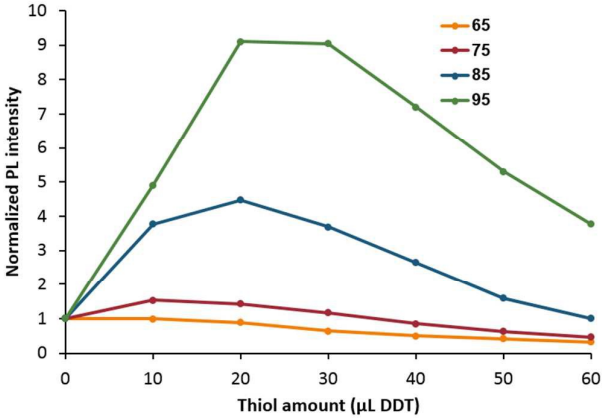

Figure 3 Photolumiscence peak intensity of 2D CdS_xSe_{1-x} nanosheets after addition of different amount of dodecanthiol (DDT).

To further investigate the surface structure we exchanged the original amine ligands with dodecanethiol. Thiol groups are known to act as hole scavengers[40] thus reducing the PL intensity. For zinc blende CdSe nanosheets, where the surface is passivated and Cd-rich,[39, 41] an addition of thiols produced significant quenching of the PL signal (Figure S6). However, the wurtzite nanostructures showed a complex behavior: small quantities of thiols yielded increased PL while higher amounts of thiols addition resulted in PL decrease (Figure 3). We attribute this phenomenon to an initial non-passivated surface of the as-synthesized nanosheets, which, by treatment with the thiols, was optimized and showed higher PL intensity. At a certain thiol concentration, the excess thiols start to act as hole scavengers and reduce the PL signal. This effect can be used to confirm the existence of surface defects on the nanosheets: the lower temperature structures show only decreased PL upon thiol addition, indicating a passivated surface as synthesized, where the thiol ligands act immediately as hole scavengers. At higher synthesis temperature, the initial enhancement of the PL intensity is more pronounced since more surface defects were present and they are being first passivated by the thiols and only later, at higher thiol concentrations, the PL decrease was seen (Figures 3 and the full dataset is presented in Figure S7). This shows that the nanosheets produced at lower temperature are more promising for photocatalysis since the generated charge is readily transferred to the hole scavengers.

Conclusions

In conclusion, we used a temperature controlled synthesis to produce CdS_xSe_{1-x} 2D nanosheets of 4-5 monolayers with tunable composition, electronic properties and surface structure. We have demonstrated that

temperature difference as small as 10°C can significantly affect the optoelectronic performance. The higher temperature synthesis yields higher Se content and possibly thicker structures (5ML), but the edge morphology shows many step defects and the surface is not passivated. In contrast, the low temperature structures have smoother edges and passivated surfaces, they contain more S (although still Se rich) and they are possibly thinner, comprising 4 ML. Using PPh_3, the emission of all samples was doubled, confirming a Se rich interface, in contrast to their zinc blende counterparts. The structures produced at 65°C appear to be fully passivated, since they immediately used thiol ligands as hole scavengers, while other samples required the use of the thiol ligands for surface passivation. Therefore, the low temperature structures are promising for the use in applications such as photocatalysis, where there is a need to eliminate surface defects.

Notes and references

‡ Footnotes relating to the main text should appear here. These might include comments relevant to but not central to the matter under discussion, limited experimental and spectral data, and crystallographic data.

§

§§

etc.

1 S. Ithurria, M. D. Tessier, B. Mahler, R. P. S. M. Lobo, B. Dubertret, A. L. Efros, *Nat. Mater.* 2011, **10**, 936.
2 F. Andrew Frame, E. C. Carroll, D. S. Larsen, M. Sarahan, N. D. Browning, F. E. Osterloh, *Chem. Comm*. 2008, **19**, 2206.
3 S. Naskar, A. Schlosser, J. F. Miethe, F. Steinbach, A. Feldhoff, N. C. Bigall, *Chem. Mater*. 2015, **27**, 3159.
4 C. E. Rowland, I. Fedin, H. Zhang, S. K. Gray, A. O. Govorov, D. V. Talapin, R. D. Schaller, *Nat. Mater.* 2015, **14**, 484.
5 E. Lhuillier, S. Pedetti, S. Ithurria, B. Nadal, H. Heuclin, B. Dubertret, *Accounts Chem. Res.* 2015, **48**, 22.
6 A. K. Geim, K. S. Novoselov, *Nat. Mater.* 2007, **6**, 183.
7 Y. Gong, J. Lin, X. Wang, G. Shi, S. Lei, Z. Lin, X. Zou, G. Ye, R. Vajtai, B. I. Yakobson, H. Terrones, M. Terrones, Beng K.Tay, J. Lou, S. T. Pantelides, Z. Liu, W. Zhou, P. M. Ajayan, *Nat. Mater.* 2014, **13**, 1135.
8 D. Jena, K. Banerjee, G. H. Xing, *Nat. Mater*. 2014, **13**, 1076.
9 X. Hong, J. Kim, S.-F. Shi, Y. Zhang, C. Jin, Y. Sun, S. Tongay, J. Wu, Y. Zhang, F. Wang, *Nat. Nanotechnol*. 2014, **9**, 682.
10 J. Xu, X. Cao, *Chem. Eng. J*, 2015, **260**, 642.
11 L. Shen, M. Luo, Y. Liu, R. Liang, F. Jing, L. Wu, *Appl. Catal. B Environm*., 2015, **166-167**, 445.
12 B. Zhu, B. Lin, Y. Zhou, P. Sun, Q. Yao, Y. Chen, B. Gao, *J. Mater. Chem. A* 2014, **2**, 3819.
13 Z. Wang, J. Hou, C. Yang, S. Jiao, H. Zhu, *Chem. Comm.* 2014, **50**, 1731.
14 D. O. Sigle, L. Zhang, S. Ithurria, B. Dubertret, J. J. Baumberg, *J. Phys. Chem. Lett.* 2015, **6**, 1099.
15 Y. Ben-Shahar, F. Scotognella, N. Waiskopf, I. Kriegel, S. Dal Conte, G. Cerullo, U. Banin, *Small* 2015, **11**, 462.
16 S. Ithurria, B. Dubertret, *J. Am. Chem. Soc*. 2008, **130**, 16504.
17 J. Joo, J. S. Son, S. G. Kwon, J. H. Yu, T. Hyeon, *J. Am. Chem. Soc.* 2006, **128**, 5632.
18 C. She, I. Fedin, D. S. Dolzhnikov, A. Demortière, R. D. Schaller, M. Pelton, D. V. Talapin, *Nano Lett.* 2014, **14**, 2772.
19 B. Guzelturk, Y. Kelestemur, M. Olutas, S. Delikanli, H. V. Demir, *ACS Nano* 2014, **8**, 6599.
20 F. Fan, P. Kanjanaboos, M. Saravanapavanantham, E. Beauregard, G. Ingram, E. Yassitepe, M. M. Adachi, O. Voznyy, A. K. Johnston, G. Walters, G.-H. Kim, Z.-H. Lu, E. H. Sargent, *Nano Lett*. 2015, **15**, 4611.
21 C. Bouet, B. Mahler, B. Nadal, B. Abecassis, M. D. Tessier, S. Ithurria, X. Xu, B. Dubertret, *Chem. Mater*. 2013, **25**, 639.
22 M. D. Tessier, P. Spinicelli, D. Dupont, G. Patriarche, S. Ithurria, B. Dubertret, *Nano Lett*. 2014, **14**, 207.
23 S. Pedetti, S. Ithurria, H. Heuclin, G. Patriarche, B. Dubertret, *J. Am. Chem. Soc.* 2014, **136**, 16430.
24 K. Wu, Q. Li, Y. Jia, J. R. McBride, Z.-x. Xie, T. Lian, *ACS Nano* 2015, **9**, 961.
25 J. S. Son, X.-D. Wen, J. Joo, J. Chae, S.-i. Baek, K. Park, J. H. Kim, K. An, J. H. Yu, S. G. Kwon, S.-H. Choi, Z. Wang, Y.-W. Kim, Y. Kuk, R. Hoffmann, T. Hyeon, *Angew. Chem. Int. Edit.* 2009, **48**, 6861.
26 Y.-H. Liu, F. Wang, Y. Wang, P. C. Gibbons, W. E. Buhro, *J. Am. Chem. Soc.* 2011, **133**, 17005.
27 Y.-H. Liu, V. L. Wayman, P. C. Gibbons, R. A. Loomis, W. E. Buhro, *Nano Lett*. 2009, **10**, 352.
28 P. S. Maiti, N. Meir, L. Houben, M. Bar-Sadan, *RSC Adv*. 2014, **4**, 49842.
29 P. S. Maiti, L. Houben, M. Bar-Sadan, *J. Phys. Chem. C* 2015, **119**, 10734.
30 A. Thibert, F. A. Frame, E. Busby, D. S. Larsen, *J. Phys. Chem. C* 2011, **115**, 19647.
31 S. J. Lim, W. Kim, S. K. Shin, *J. Am. Chem. Soc.* 2012, **134**, 7576.
32 J. S. Son, K. Park, S. G. Kwon, J. Yang, M. K. Choi, J. Kim, J. H. Yu, J. Joo, T. Hyeon, *Small* 2012, **8**, 2394.
33 T. Aubert, M. Cirillo, S. Flamee, R. Van Deun, H. Lange, C. Thomsen, Z. Hens, *Chem. Mater*. 2013, **25**, 2388.
34 J.-P. Kim, J. A. Christians, H. Choi, S. Krishnamurthy, P. V. Kamat, *J. Phys. Chem. Lett*. 2014, **5**, 1103.
35 C. Landes, M. Braun, C. Burda, M. A. El-Sayed, *Nano Lett*. 2001, **1**, 667.
36 T. E. Rosson, S. M. Claiborne, J. R. McBride, B. S. Stratton, S. J. Rosenthal, *J. Am. Chem. Soc.* 2012, **134**, 8006.
37 S. Dolai, P. R. Nimmala, M. Mandal, B. B. Muhoberac, K. Dria, A. Dass, R. Sardar, *Chem. Mater*. 2014, **26**, 1278.
38 J. Jasieniak, P. Mulvaney, J. Am. Chem. Soc. 2007, 129, 2841.
39 E. Baghani, S. K. O'Leary, I. Fedin, D. V. Talapin, M. Pelton, *J. Phys. Chem. Lett.* 2015, **6**, 1032.
40 A. Zhang, C. Dong, H. Liu, J. Ren, *J. Phys. Chem. C* 2013, **117**, 24592.
41 E. M. Hutter, E. Bladt, B. Goris, F. Pietra, J. C. van der Bok, M. P. Boneschanscher, C. de Mello Donegá, S. Bals, D. Vanmaekelbergh, *Nano Lett*. 2014, **14**, 6257.

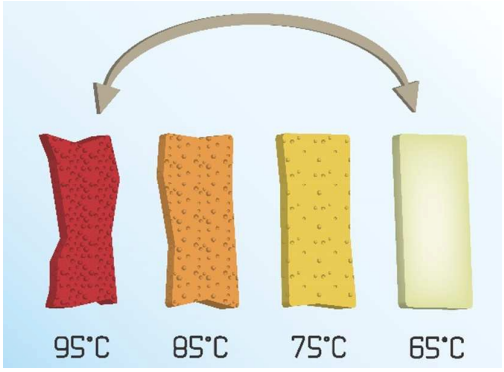

Surface engineering and tuning of the optoelectronic properties of wurtzite CdS_xSe_{1-x} nanosheets by ligand exchange